Available online at www.sciencedirect.com

jmr&t Journal of Materials Research and Technology

journal homepage: www.elsevier.com/locate/jmrt

Aluminum based high temperature thin film electrode system for wireless sensors

*Marietta Seifert**, *Barbara Leszczynska*, *Siegfried B. Menzel*, *Hagen Schmidt*, *Thomas Gemming*

Leibniz Institute for Solid State and Materials Research, Helmholtzstr. 20, 01069 Dresden, Germany

ARTICLE INFO

Article history:
Received 2 June 2023
Accepted 4 August 2023
Available online 9 August 2023

Keywords:
High-temperature sensing
SAW device
Aluminum ruthenium alloy electrodes
AlRu
RuAl
CTGS

ABSTRACT

Self-sustained, wireless high-temperature stable sensors are developed, which are based on an aluminum alloy as the electrode metallization. Due to its cost-effectiveness accompanied by a high-temperature stability, this alloy substitutes and outperforms the commonly applied expensive Pt- and Ir-based metals. For the first time, a comprehensive structural, electrical and high-frequency characterization of these surface acoustic wave (SAW) sensors is shown. They are based on Catangasite ($Ca_3TaGa_3Si_2O_{14}$, CTGS) in combination with properly structured cover and barrier layers for the metallization. The frequency characteristics is determined up to 700 °C by ex situ and in situ methods. In addition, the morphology of the AlRu electrodes is analyzed after the thermal loadings and the temperature dependent sheet resistance is measured. The results reveal a reproducible and linear correlation between the applied temperature and the sheet resistance as well as the resonant frequency. In addition, hardly any degradation of the electrodes is detected after the thermal loadings. The observed high-temperature stability of the devices up to at least 700 °C demonstrates the large potential of the AlRu based SAW sensors as a cost-efficient alternative to expensive noble metal based sensors in industrial applications for the support of energy efficient operation.

© 2023 The Author(s). Published by Elsevier B.V. This is an open access article under the CC BY license (http://creativecommons.org/licenses/by/4.0/).

1. Introduction

Energy efficient industrial processes require a precise knowledge and control of process temperatures, especially at high temperatures. Therefore, there is a large demand for high-temperature in situ monitoring of devices, component parts, and processes to control and optimize temperature critical fabrication procedures and energy consumption. This demand is also driven from the demands of highly automated and reliable production systems of future factories based on industry 4.0. Furthermore, the knowledge on physical or chemical parameters, e.g., the exact temperature, pressure or presence of gases, is a prerequisite to realize an energy saving operation with high reproducibility and accuracy. Sensors based on piezoelectric materials offer many opportunities [1]. However, it is not possible to access all locations of interest with common wired sensors so that more advanced wireless sensing solutions are needed. One suited option to realize such measurements is the application of a sensor based on surface acoustic waves (SAW) [2]. Additionally, self-powered sensors without the need for an internal power supply are most suited for self-sustaining

* Corresponding author.
E-mail address: marietta.seifert@ifw-dresden.de (M. Seifert).

https://doi.org/10.1016/j.jmrt.2023.08.025

2238-7854/© 2023 The Author(s). Published by Elsevier B.V. This is an open access article under the CC BY license (http://creativecommons.org/licenses/by/4.0/).

wireless sensors as they need less components compared to built-in generators [3].

Such passive SAW based sensors deploy the basic working principle of the transformation of a high frequency electric signal in a SAW through a specific array of two interdigitated comb-shaped finger electrodes on a piezoelectric substrate. Fig. 1 demonstrates two main operation principles of SAW based sensors. The schematic architecture of a SAW based reflective delay line sensor tag including a base plate or chip carrier, an antenna, and electrical connection lines between the contact pads of the SAW sensor tag and the antenna is shown in Fig. 1a.

The measurement principle of a temperature sensor based on a SAW resonator is a reversible temperature dependent shift of the resonant frequency of the device. The known correlation between the temperature of the device and the value of its resonant frequency allows the calculation of the temperature the sensor is faced with based on the measured electrical frequency characteristics (Fig. 1b).

Such wireless sensors can be applied, e.g., in rotating gas and steam turbines or heating systems to monitor and, based on this, to optimize the processes, and therefore, these sensors will support an efficient service. However, to enable high operation temperatures, a high-temperature stability of all materials, of which the SAW sensor is composed, is crucial. That implies the use of a high-temperature stable piezoelectric substrate in combination with a high-temperature stable electrode metallization. Up to now, research mainly concentrated on noble metal electrodes, such as Pt-, Pd- or Ir-based materials, and on Langasite ($La_3Ga_5SiO_{14}$, LGS) substrates [4–12].

Besides LGS, Catangasite ($Ca_3TaGa_3Si_2O_{14}$, CTGS), a more ordered member of the same crystal family, is another promising high-temperature stable piezoelectric substrate for application in SAW devices [13–17]. However, only few literature is available on SAW devices on CTGS substrates, and in these cases, noble metal electrodes were used to determine the elastic properties of the piezoelectric crystal rather for sensing purposes [18,19].

Due to their high costs, SAW devices with noble metal electrodes are not desired for industrial mass production and alternatives with lower costs are strongly favored. One such alternative electrode metallization with significant high temperature capability is the investigated AlRu alloy (density: about 8 g/cm^3, Young's modulus: 267 GPa [20]). During the last years, a temperature-stable AlRu layer system equipped with suited cover and barrier layers on CTGS substrates was developed [21–24].

However, up to now, investigations on AlRu thin films for the application in SAW sensors were restricted to short-term high-temperature experiments of extended films and the characterization of their film morphology and resistivity after certain heat treatments. In situ experiments at elevated temperatures haven't been performed yet. In contrast to the extended films, SAW devices possess a large number of edges of the individual electrodes. As these are crucial for the SAW device operation and might alter the behavior of the device as compared to an infinite film, particular investigations are required. Therefore, for the first time, this paper presents a comprehensive structural, electrical and high-frequency characterization of SAW sensors with AlRu electrodes to evaluate their suitability for high-temperature applications.

2. Materials and methods

AlRu based SAW temperature sensors were prepared by deposition of a multilayer of two times 55 nm of AlRu in-between three layers of 7 nm of Al on piezoelectric $Ca_3TaGa_3Si_2O_{14}$ (CTGS, Y-cut with X-propagation; Euler angles (0°, −90°, 0°)) substrates by magnetron sputtering from elemental targets. This optimized layer stack resulted from former experiments [24]. To prevent a chemical reaction between the CTGS and the metallization, a barrier layer consisting of 20 nm SiO_2 and 20 nm AlNO was included into the layer stack (for details of deposition of the barrier layers see [24]). In the next step, the layer stack was coated with a resist, in which the layout of the SAW devices was structured via photolithography. This step was performed in cooperation with SAW Components Dresden. Subsequently, ion beam etching of the electrode metallization was used to pattern the SAW devices. After the structuring, the devices were covered with 20 nm of SiO_2 and 20 nm of AlNO.

The electrical resistance along the plane of the extended films as a function of temperature was measured with a home-built oven setup by contacting the sample with a size of 23 by 24 mm with 4 platinum tips. This electrical sheet resistance is denoted as R_S in Ω per square (Ω/□) and was

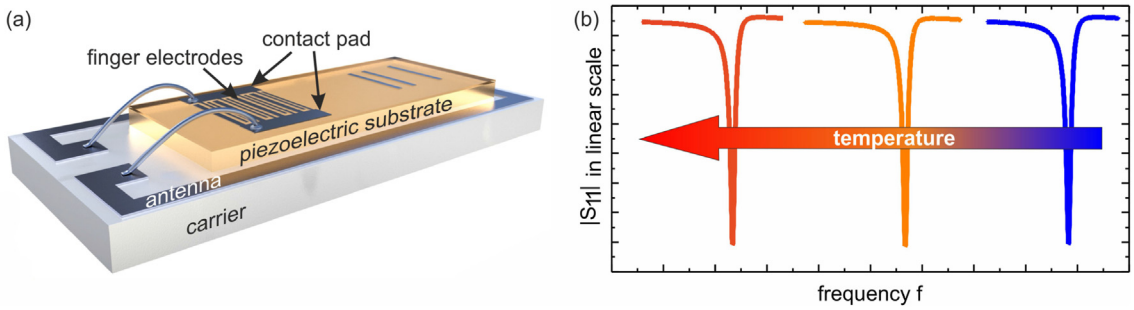

Fig. 1 – Example of SAW based sensor devices: (a) schematic architecture of a SAW based reflective delay line sensor tag, (b) principle operation of a temperature sensor based on a SAW resonator in terms of the reversible shift of its electrical frequency characteristics $|S_{11}|$.

determined using the van der Pauw method [25]. The heating rate was 6 Kmin^{-1} and the cooling proceeded passively, i.e., by self-cooling down.

Transmission electron microscopy (TEM) investigations were performed with a Technai F30 (FEI company, Hillsboro, OR, USA). Energy dispersive X-ray spectroscopy (EDX) was used to reveal the chemical composition and to search for oxidation.

The electrical high-frequency behavior of the AlRu based SAW sensors was characterized via $|S_{11}|$-parameter measurements. Two kinds of measurements were performed. Samples were characterized at room temperature prior and after a thermal loading at 700 °C using a vector network analyzer (VNA, Keysight E5080B). In a second experiment, the sensors were connected to a Pt wire dipole antenna and the electrical measurement was done wirelessly during an in situ annealing of the devices, so that the temperature dependent characteristics could be observed.

3. Results

3.1. Measurement of the electrical sheet resistance

A fundamental requirement, mandatory for the reproducible application of high-temperature sensors, is a low and stable electrical resistivity of the electrode metallization. Measurements of the electrical sheet resistance of an extended AlRu film with a thickness of 131 nm with cover and barrier layers on CTGS were repeatedly performed in situ up to 800 °C in high vacuum (HV) and in air, respectively. In each cycle, the sample was kept at 800 °C for 6 h. The results of the respective in situ van der Pauw measurements are shown in Fig. 2.

At the beginning of the temperature treatments, a rather high sheet resistance of 5.7 Ω per square (Ω/□) was measured at room temperature (RT). With increasing temperature up to about 200 °C, there was a small increase in sheet resistance, followed by a strong increase up to a maximum value of 10.7 Ω/□ at 450 °C (Fig. 2a). Then, up to the maximum temperature of 800 °C, the sheet resistance decreased continuously and finally reached 4.4 Ω/□. During the thermal loading for 6 h at 800 °C, there was a slight further decrease of the sheet resistance to 3.8 Ω/□. Fig. 2b demonstrates that this drop of the sheet resistance during the isothermal annealing at 800 °C occurred within the first 10 min after reaching this temperature, followed by an almost stable state. The passive cooling down to RT led to a linear decrease of the sheet resistance. For all subsequent temperature cycles (i.e. 2–5), the courses of the heating curves were similar to those of the cooling curves so that for reasons of clarity, only the cooling parts of these further cycles are plotted in Fig. 2a. It can be seen that they were almost identical with a further total decrease of the sheet resistance at 800 °C of only 2%. In contrast to this, the cooling curves of the first five temperature cycles of an AlRu sample measured in air showed a slightly stronger decrease of about 4% (Fig. 2c). The temperature coefficient of resistance (TCR) extracted from the cooling curves (800 °C down to 20 °C) was 24.2 · 10^{-4} K^{-1} and 26.5 · 10^{-4} K^{-1} for the HV and air sample, respectively. These values were in good agreement with the TCR value between 20.5 · 10^{-4} K^{-1} and 22.7 · 10^{-4} K^{-1} determined by Smith and Lang for bulk AlRu [26]. The final resistivity of the films measured at room temperature was about 16 μΩcm and with this corresponds to the values reported in [24].

The strong increase in sheet resistance during the first heating above about 200 °C can be explained with the onset of the interdiffusion of the pure, low resistivity Al layers with the AlRu within the Al–AlRu layer stack. It is assumed that the formation of the AlRu phase, grain growth and the reduction of defects led to the decrease of the sheet resistance above 450 °C. Similar effects were expected to cause the reduction of the sheet resistance during the thermal loadings at 800 °C.

The slightly stronger decrease of the sheet resistance of the air annealed sample as compared to the HV sample after the

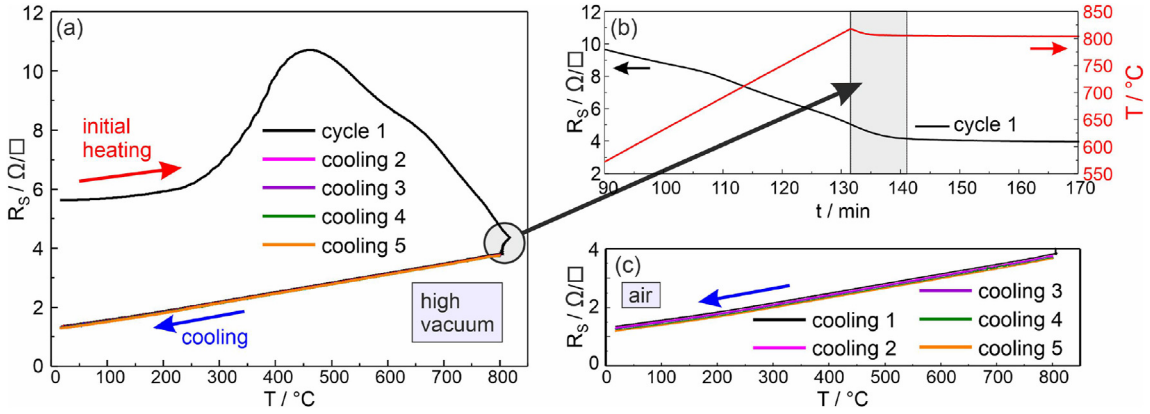

Fig. 2 – In situ measured electrical sheet resistance R_S of the investigated AlRu films: (a) in HV, initial (first) complete temperature cycle comprising heating (heating rate: 6 Kmin^{-1}) and cooling as well as the cooling sequence of the 4 subsequent cycles. Note the overlap of all five cooling curves. The dwell time at 800 °C was 6 h for each cycle. (b) Sheet resistance and temperature in dependence on the annealing time for the first heating, section between 90 and 170 min. (c) Cooling sequences of 5 temperature cycles for a sample measured in air (the corresponding heating curve shows a behavior similar to the HV annealed sample).

whole annealing procedure might be ascribed to a partly oxidation of Al in the air atmosphere, which led to the formation of pure Ru grains with a lower resistivity as compared to AlRu.

Although the observed reduction of the sheet resistance at 800 °C was almost negligible, the subsequent experiments were carried out up to the maximum temperature of 700 °C to avoid this degradation. Furthermore, a maximum operation temperature of 700 °C comprises most relevant applications, as, e.g., steam turbines or parts of combustion chambers of mobile heating systems.

3.2. *Characterization of the morphology*

An AlRu based SAW sensor was thermally loaded for 192 h at 700 °C in air to determine the high temperature stability of the metallization regarding morphology and potential degradation. To reveal if the edges of the electrodes act as starting points for a degradation or oxidation during the high temperature operation, a detailed TEM investigation was performed for finger electrodes as well as for the extended contact pads. The TEM image of the finger electrode in Fig. 3a showed a homogeneous morphology. EDX measurements revealed the presence of pure Ru at the edges of the fingers. The major part of the fingers consisted of AlRu with a stoichiometric composition of about 50:50 at.%. In addition, there were a few individual Ru grains at the upper interface of the metallization. Between the metallization and the SiO_2 cover layer, a 30 nm thick layer consisting of an aluminum-silicon-oxide was present, which was formed during the thermal loading by a chemical reaction between the Al of the AlRu and the SiO_2 cover layer. Its composition was close to that of Al_2SiO_5 or $Al_6Si_2O_{13}$ and is therefore denoted as Al_xSiO_y here. This chemical reaction resulted in a lack of Al for the formation of the AlRu phase, which explained the consequent presence of pure Ru grains. The dominant presence of Ru at the edges of the finger could be explained with a stronger oxidation of Al at these positions due to the reduced thickness of the cover layers there, which enabled an inwards diffusion of oxygen from the ambient atmosphere.

Compared with the finger electrode, the contact pad contained less grains of pure Ru and the thickness of the Al_xSiO_y layer was slightly lower with just 25 nm (Fig. 3b). In contrast, the contact pad contained small pores within the AlRu metallization. To demonstrate the influence of the thermal loading on the morphology, a cross section of the as-prepared electrode metallization consisting of a multilayer of 3 times 7 nm Al which comprise two AlRu layers with 55 nm thickness between them is shown in Fig. 3c. The multilayer structure and the nanocrystalline morphology are clearly visible.

In summary, the long-term thermal loading only led to a minor degradation of the electrodes, which was slightly different in the finger electrodes as compared to the contact pad due to effects at the edges. In standardized industrial processes, the deposition of the cover layers will be optimized to realize a constant thickness of the protecting layer at all positions, e.g., by methods like atomic layer deposition, to achieve an even better stability.

The results also demonstrated that prior to an application, a formation annealing of the sensor is required to adjust the intended morphology and to reach the low resistivity of the electrode metallization. This formation annealing was performed for all samples under investigation at 800 °C in ultra-high vacuum for 10 h. The temperature was chosen higher than the intended application temperature of 700 °C to avoid further changes of the morphology during operation, even on a long-term scale.

3.3. *Electrical characteristics of the SAW device*

The electrical high-frequency response of the AlRu based sensor measured at RT after the formation annealing at 800 °C in ultra-high vacuum for 10 h is shown in Fig. 4. To enable the measurements using a wafer prober, a 50 nm thick Pt layer was deposited as probing promoter on top of the contact pads after the formation annealing to ensure reliable probing with

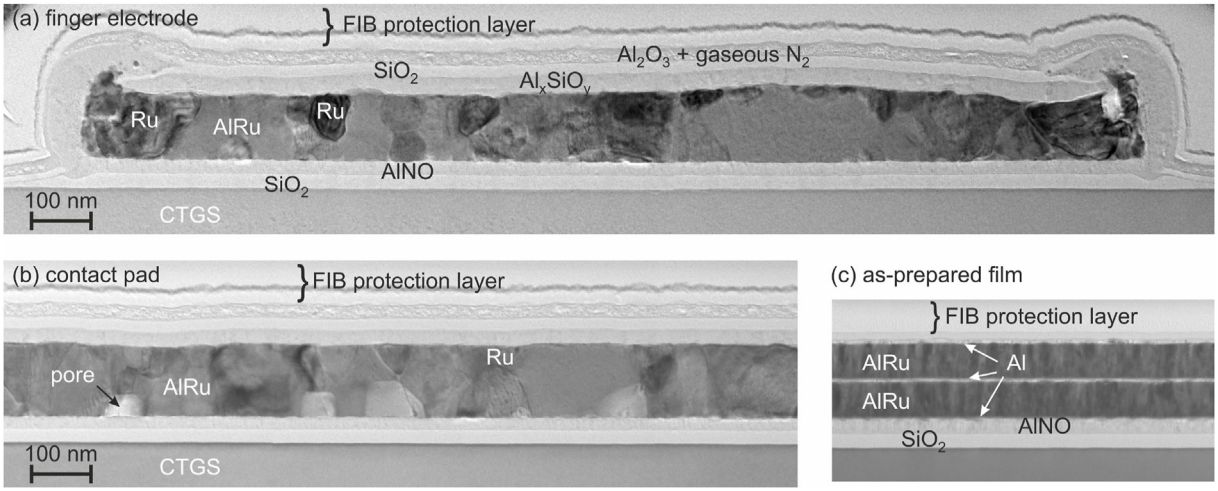

Fig. 3 – TEM images (cross sections) of the AlRu metallization system of the SAW sensor (a) finger electrode, (b) contact pad, both after thermal loading at 700 °C for 192 h in air, (c) in the as-prepared state without cover layers.

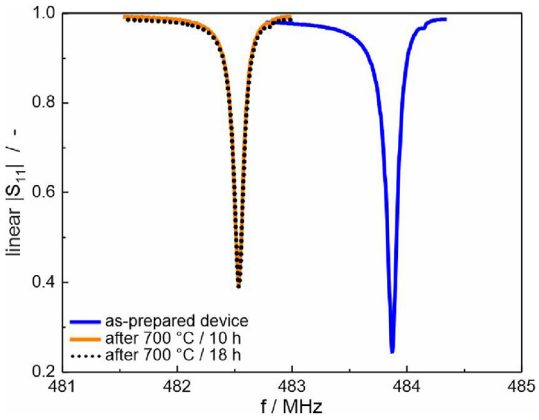

Fig. 4 – Room temperature high-frequency characteristic of the SAW device with AlRu metallization in terms of the linear reflection coefficient $|S_{11}|$ in the as-prepared state, after the first thermal loading of the formation annealed structure with as-deposited Pt probing promoter at 700 °C in air for 10 h and after a second thermal loading in air at 700 °C for 8 h.

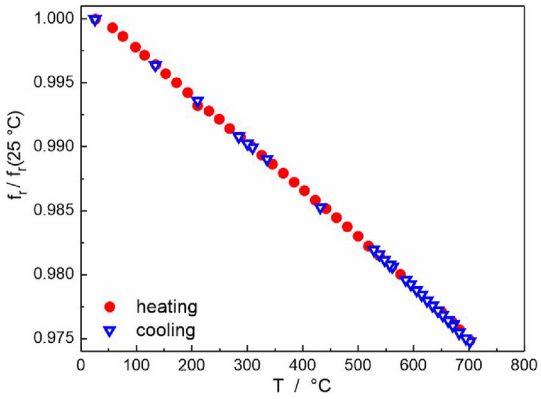

Fig. 5 – Fully reversible shift of the resonant frequency f_r normalized to 25 °C of an AlRu based sensor in dependence on the temperature measured in situ in air atmosphere inside the furnace by wireless interrogation after a pre-conditioning of the whole device at 700 °C for 2 h.

standard RF probe tips. A high quality of the $|S_{11}|$ curve was observed for all devices, which was not adversely affected by the thin insulating barrier layers due to relatively low dielectric constants and coupling coefficient of the high-temperature CTGS cystal [27] when compared to piezoelectric substrates like $LiNbO_3$. After initial probing, the sensor was thermally loaded at 700 °C for 10 h in air and evaluated again at RT. This heat treatment led to a shift of the resonant frequency to a lower value. However, after a subsequent second thermal loading at 700 °C in air for 8 h, no further change of the frequency response was measured, proving the stability of the device.

The shift of the resonant frequency after the first thermal loading was ascribed to changes of the morphology of the Pt probing promoter, deposited here to provide easy characterization by the probe tips. Light microscopy images revealed a strong increase in surface roughness of the Pt layer after the first thermal loading. Pt films are known to easily agglomerate at high temperatures, which could explain the increase in the surface roughness. In addition, the electrical properties of the Pt layer changed during the heat treatment due to grain growth and healing of defects. These effects led to a change in the electrical loss of the structure and hereby to the observed change of the resonant frequency. Obviously, the conditioning of the Pt layer was finalized within the first 10 h of thermal loading at 700 °C, so that the further heat treatment did not yield a further shift. This result proved the suitability of AlRu based sensors for applications at least up to 700 °C in air.

The underlying working principle of a temperature sensor based on a SAW device is an unambiguous, at best linear, dependence of the resonant frequency on the applied temperature. To prove the suitability of the AlRu metallization for real sensor applications, the temperature dependent reversible change of the resonant frequency of an AlRu based SAW device was determined by wireless interrogation of the sensor connected by Pt wire bonding to a Pt wire dipole antenna. The whole device including the antenna was then placed into a tube furnace in air and the temperature was increased up to 700 °C. A first temperature cycle up to 700 °C with a dwell time of 2 h at this temperature served as a thermal pre-conditioning of the bond connections and the antenna. After this process, during the wireless interrogation by means of a butterfly antenna placed 20 cm away from the tube furnace, the SAW device showed a linear correlation between the temperature and the normalized resonant frequency during heating and cooling (Fig. 5). Only at temperatures above 600 °C, a slight deviation of the curve from a linear behavior was observed. This observation corresponded well with the results of Yang et al., who investigated the frequency–temperature response of a SAW sensor on CTGS at temperatures up to 1100 °C. They observed a quadratic relation for the whole temperature range, which also led to a stronger decrease of the resonant frequency when the temperature was increased above 600 °C [19]. In the linear regime between 100 °C and 600 °C, an evaluation of the slope resulted in -36.7 ppm K^{-1}, demonstrating the capability of AlRu electrode systems on CTGS for high-temperature operation.

4. Conclusion

This paper presents a holistic investigation of SAW sensors with aluminum based electrodes comprising analyses of their morphology by TEM measurements and of the electrical characteristics by means of $|S_{11}|$ ex situ and in situ temperature dependent methods up to 700 °C. An almost negligible oxidation of the electrodes was observed and reproducible frequency characteristics after thermal loading were realized. The linear and reproducible correlation between the temperature and the electrical resistivity of extended AlRu films as well as between the temperature and the resonant frequency of the SAW devices emphasize the huge potential of the AlRu

sensor metallization for applications up to at least 700 °C in air. It is expected that even higher temperatures can be reached in less oxidizing atmospheres, since former experiments in high vacuum up to 900 °C on extended films proved a stability of the films in these conditions [24]. Due to its industry-compatible material composition and technology and the low costs, the AlRu metallization is a promising alternative to expensive Pt-, Pd- or Ir-based sensors for use in steam turbines or in heating systems, respectively, to optimize the processes and therefore to improve an energy-saving operation.

Data availability

The raw/processed data required to reproduce these findings cannot be shared at this time as the data also forms part of an ongoing study.

Declaration of Competing Interest

The authors declare that they have no known competing financial interests or personal relationships that could have appeared to influence the work reported in this paper.

Acknowledgements

The work was supported by German BMWI (03ET1589 A) and DFG (470028346). The authors gratefully acknowledge Andreas Büst for thin film deposition, and Thomas Wiek and Dina Bieberstein for SEM images and TEM lamella preparation. Open access publication was partly funded by the Open Access Fund of the Leibniz Association.

REFERENCES

[1] Zida SI, Lin Y-D, Khung YL. Current trends on surface acoustic wave biosensors. Advan Mater Technol 2021;6(6):2001018. https://doi.org/10.1002/admt.202001018.
[2] Yang Y, Mengue P, Mishra H, Floer C, Hage-Ali S, Petit-Watelot S, et al. Wireless multifunctional surface acoustic wave sensor for magnetic field and temperature monitoring. Advan Mater Technol 2022;7(3):2100860. https://doi.org/10.1002/admt.202100860.
[3] Chen B, Tang W, Wang ZL. Advanced 3d printing-based triboelectric nanogenerator for mechanical energy harvesting and self-powered sensing. Mater Today 2021;50:224–38. https://doi.org/10.1016/j.mattod.2021.05.017.
[4] Moulzolf S, Frankel D, Pereira da Cunha M, Lad R. High temperature stability of electrically conductive Pt–Rh/ZrO_2 and Pt–Rh/HfO_2 nanocomposite thin film electrodes. Microsyst Technol 2014;20(4–5):523–31. https://doi.org/10.1007/s00542-013-1974-x.
[5] Liu X, Peng B, Zhang W, Zhu J, Liu X, Wei M. Improvement of high-temperature stability of Al_2O_3/Pt/ZnO/Al_2O_3 film electrode for saw devices by using Al_2O_3 barrier layer. Materials 2017;10(12):1377. https://doi.org/10.3390/ma10121377.
[6] Moreira ADSL, Bartasyte A, Belharet D, Soumann V, Margueron S, Broenner A. Stabilized Pt interdigitated electrodes for high-temperature SAW sensors. In: 2021 IEEE International Ultrasonics Symposium (IUS); 2021. p. 1–4. https://doi.org/10.1109/IUS52206.2021.9593767.
[7] Zhou X, Tan Q, Liang X, Lin B, Guo T, Gan Y. Novel multilayer SAW temperature sensor for ultra-high temperature environments. Micromachines 2021;12(6):643. https://doi.org/10.3390/mi12060643.
[8] Xue T, Xu F, Tan Q, Yan X, Liang X. LGS-based SAW sensor that can measure pressure up to 1000 °C. Sensor Actuator Phys 2022;334:113315. https://doi.org/10.1016/j.sna.2021.113315.
[9] Aubert T, Bardong J, Elmazria O, Bruckner G, Assouar B. Iridium interdigital transducers for high-temperature surface acoustic wave applications. IEEE Trans Ultrason Ferroelectr Freq Control 2012;59(2):194–7. https://doi.org/10.1109/TUFFC.2012.2178.
[10] Thiele JA, da Cunha MP. Platinum and palladium high-temperature transducers on langasite. IEEE Trans Ultrason Ferroelectr Freq Control 2005;52(4):545–9. https://doi.org/10.1109/TUFFC.2005.1428035.
[11] Sakharov S, Zabelin A, Medvedev A, Buzanov O, Kondratiev S, Roshchupkin D, et al. Technological process and resonator design optimization of Ir/LGS high temperature SAW devices. In: Proceedings of the 2014 IEEE International Ultrasonics Symposium Proceedings Chicago, IL, USA; 2014. p. 1632–5. https://doi.org/10.1109/ULTSYM.2014.0093. 3–6 September 2014.
[12] Taguett A, Aubert T, Elmazria O, Bartoli F, Lomello M, Hehn M, et al. Comparison between Ir, $Ir_{0.85}Rh_{0.15}$ and $Ir_{0.7}Rh_{0.3}$ thin films as electrodes for surface acoustic waves applications above 800 °C in air atmosphere. Sensor Actuator Phys 2017;266:211–8. https://doi.org/10.1016/j.sna.2017.09.031.
[13] Suhak Y, Schulz M, Johnson WL, Sotnikov A, Schmidt H, Fritze H. Electromechanical properties and charge transport of $Ca_3TaGa_3Si_2O_{14}$ (CTGS) single crystals at elevated temperatures. Solid State Ionics 2018;317:221–8. https://doi.org/10.1016/j.ssi.2018.01.032.
[14] Biryukov SV, Schmidt H, Sotnikov A, Weihnacht M, Sakharov S, Buzanov O. CTGS material parameters obtained by versatile SAW measurements. In: 2014 IEEE International Ultrasonics Symposium; 2014. p. 882–5. https://doi.org/10.1109/ULTSYM.2014.0217.
[15] Suhak Y, Fritze H, Sotnikov A, Schmidt H, Johnson WL. High-temperature electromechanical loss in piezoelectric langasite and catangasite crystals. J Appl Phys 2021;130(8):085102. https://doi.org/10.1063/5.0058751.
[16] Seifert M, Leszczynska B, Weser R, Menzel S, Gemming T, Schmidt H. Durability of TiAl based surface acoustic wave devices for sensing at intermediate high temperatures. J Mater Res Technol 2023;23:4190–8. https://doi.org/10.1016/j.jmrt.2023.02.070.
[17] Weihnacht M, Sotnikov A, Suhak Y, Fritze H, Schmidt H. Accuracy analysis and deduced strategy of measurements applied to $Ca_3TaGa_3Si_2O_{14}$ (CTGS) material characterization. In: 2017 IEEE International Ultrasonics Symposium (IUS); 2017. https://doi.org/10.1109/ULTSYM.2017.8092822. 1–1.
[18] Sakharov S, Zabelin A, Medvedev A, Bazalevskaya S, Buzanov O, Kondratiev S, et al. Investigation of the CTGS single crystals potential for high temperature SAW devices. In: 2013 IEEE International Ultrasonics Symposium (IUS); 2013. p. 1085–8. https://doi.org/10.1109/ULTSYM.2013.0278.
[19] Yang Y, Peng B, Yue H, Huang F, He P, He Z, et al. Temperature characteristics of surface acoustic wave resonators prepared on (0°, 90°, ψ) CTGS cuts. Appl Acoust

2022;194:108788. https://doi.org/10.1016/j.apacoust.2022.108788.
[20] Mucklich F, Ilic N. RuAl and its alloys. Part I. Structure, physical properties, microstructure and processing. Intermetallics 2005;13(1):5–21. https://doi.org/10.1016/j.intermet.2004.05.005.
[21] Seifert M, Menzel SB, Rane GK, Hoffmann M, Gemming T. RuAl thin films on high–temperature piezoelectric substrates. Mater Res Express 2015;2(8):085001. https://doi.org/10.1088/2053-1591/2/8/085001.
[22] Seifert M, Rane GK, Menzel SB, Oswald S, Gemming T. Improving the oxidation resistance of RuAl thin films with Al_2O_3 or SiO_2 cover layers. J Alloys Compd 2019;776:819–25. https://doi.org/10.1016/j.jallcom.2018.10.278.
[23] Seifert M, Brachmann E, Rane GK, Menzel SB, Oswald S, Gemming T. Pt-RuAl bilayers as a model system for Pt wire bonding of high-temperature RuAl electrodes. J Alloys Compd 2020;813:152107. https://doi.org/10.1016/j.jallcom.2019.152107.
[24] Seifert M. High temperature behavior of RuAl thin films on piezoelectric CTGS and LGS substrates. Materials 2020;13(7). https://doi.org/10.3390/ma13071605.
[25] van der Pauw LJ. A method of measuring specific resistivity and Hall effect of discs of arbitrary shape. Philips Res Rep 1958;13:1–9.
[26] Smith EG, Lang CI. High temperature resistivity and thermo-EMF of RuAl. Scripta Metall Mater 1995;33(8):1225–9. https://doi.org/10.1016/0956-716X(95)00374-5.
[27] Sotnikov A, Schmidt H, Weihnacht M, Buzanov OA, Sakharov S. Material parameters of $Ca_3TaGa_3Si_2O_{14}$ single crystal revisited. In: 2013 IEEE International Ultrasonics Symposium (IUS); 2013. p. 1688–91.